Topological Ferrimagnetic Behavior of Two New $[Mn(L)_2(N_3)_2]_n$ Chains with the New AF/AF/F Alternating Sequence (L = 3-Methylpyridine or 3,4-Dimethylpyridine)

Morsy A. M. Abu-Youssef,[†] Marc Drillon,[‡] Albert Escuer,*[,§] Mohamed A. S. Goher,[†] Franz A. Mautner,[||] and Ramon Vicente[§]

Chemistry Department, Faculty of Science, Alexandria University, P.O. Box 426, Ibrahimia, Alexandria 21321, Egypt, Institut de Physico-Chimie des Materiaux CNRS Strasbourg, UMR 75040, F-67037, Strasbourg, France, Departament de Química Inorgànica, Universitat de Barcelona, Diagonal 647, 08028, Barcelona, Spain, and Institut für Physikalische und Theoretische Chemie, Technische Universität Graz, A-8010 Graz, Austria

Received May 16, 2000

The reaction of manganese(II) and pyridine derivatives such as 3-methylpyridine (3-Mepy) and 3,4-dimethylpyridine (3,4-Dmepy) led to the new one-dimensional systems *trans*-$[Mn(3\text{-Mepy})_2(N_3)_2]_n$ (**1**) and *trans*-$[Mn(3,4\text{-Dmepy})_2(N_3)_2]_n$ (**2**). Compound **1** crystallizes in the monoclinic system, space group $P2_1/n$, $a = 11.201(3)$ Å, $b = 14.499(4)$ Å, $c = 14.308(4)$ Å, $Z = 6$, and compound **2** crystallizes in the triclinic system, space group $P\bar{1}$, $a = 11.502(4)$ Å, $b = 14.246(5)$ Å, $c = 16.200(8)$ Å, $Z = 6$. The two compounds show the same general one-dimensional arrangement of double azido bridges between neighboring manganese atoms with the unprecedented $-Mn-(\mu_{1,3}\text{-}N_3)_2-Mn-(\mu_{1,3}\text{-}N_3)_2-Mn-(\mu_{1,1}\text{-}N_3)_2-Mn-$ sequence. Susceptibility and magnetization measurements reveal a ferrimagnetic-like behavior derived from the topology of the chain. A model of the Heisenberg chain, comprising classical spins coupled through alternating exchange interactions $J_1J_1J_2...$ is proposed to describe the magnetic behavior.

Introduction

Polynuclear azido-bridged derivatives are a rich source of new magnetic systems thanks to the extreme versatility of the coordination modes of the azido ligand,[1] which may coordinate as $\mu_{1,3}$-N_3 (end-to-end, EE), $\mu_{1,1}$-N_3 (end-on, EO), or even in more exotic modes as $\mu_{1,1,1}$-N_3 or $\mu_{1,1,3}$-N_3.[2,3] The similar degree of stability of the EE or EO coordination modes often favors a variety of topologies or dimensionalities as a result of minor changes in the manganese environment, as has largely been reported for compounds with general formula $[Mn(L)_2(N_3)_2]_n$, (L = two monodentate or one LL bidentate pyridinic derivatives).[1]

Packing forces may also be a determinant factor in the coordination of the azido ligand, as has been shown in the case of compounds with general formula $C^+[Mn(N_3)_3]^-$ in which 1-D or 3-D dimensionality and EE, EO, or alternating EE−EO coordination have been reported as being related to the size of the countercation C^+.[2,4] In addition to the structural possibilities, the common antiferromagnetic (AF) interaction in the EE mode and the ferromagnetic (F) coupling generally found in the EO mode[1,5] offer exciting research prospects for magnetochemists.

Focusing on the one-dimensional Mn^{II} azido compounds, six different topologies have been found to date for the $[Mn(L)_2(N_3)_2]_n$ derivatives (Chart 1): ferromagnetic chains[6] with double EO azido bridges (topology **A**) with L = 2-benzoylpyridine;[6a] antiferromagnetic chains with double EE bridges (topology **B**) with L = 3-ethylpyridine, 2- hydroxipyridine,[7] and 3,5-dimethylpyridine;[6a] AF/F alternating systems (topology **C**) with LL = 2,2′-bipyridyl[8] and L = 3-benzoylpyridine[6a] or 3-ethyl,4-methylpyridine;[9] with different stoichiometry, AF/F alternating systems (topology **D**) with L = 3-aminopyridine or the cationic chain with L = 3-ethyl-4-methylpyridine and hexafluorophosphate as counteranion;[10] more exotic topologies with complex alternating patterns have been recently reported (**E** and **F**).[11]

Continuing with the systematic exploration of the effect of the ancillary pyridinic ligands, we report the synthesis, structural determination, and study of the magnetic properties of two new members of the $[Mn(L)_2(N_3)_2]_n$ series, with formula *trans*-$[Mn(3\text{-Mepy})_2(N_3)_2]_n$ (**1**) and *trans*-$[Mn(3,4\text{-Dmepy})_2(N_3)_2]_n$ (**2**) in which 3-Mepy and 3,4-Dmepy correspond to the 3-methylpyridine and 3,4-dimethylpyridine, respectively. These two compounds share the common features of one-dimensional systems bridged by double azido bridges but with the EE/EE/EO

[†] Alexandria University.
[‡] Institut de Physico-Chimie des Materiaux, CNRS Strasbourg.
[§] Universitat de Barcelona.
[||] Technische Universität Graz.

(1) Ribas, J.; Escuer, A.; Monfort, M.; Vicente, R.; Cortés, R.; Lezama, L.; Rojo, T. *Coord. Chem. Rev.* **1999**, *193*−*195*, 1027.
(2) Goher, M. A. S.; Cano, J.; Journaux, Y.; Abu-Youssef, M. A. M.; Mautner, F. A.; Escuer, A.; Vicente, R. *Chem.*− *Eur. J.* **2000**, *6*, 778.
(3) Ribas, J.; Monfort, M.; Solans, X.; Drillon, M. *Inorg. Chem.* **1994**, *33*, 742.
(4) Mautner, F. A.; Cortés, R.; Lezama, L.; Rojo, T. *Angew. Chem.* **1996**, *108*, 96; *Angew. Chem., Int. Ed. Engl.* **1996**, *35*, 78.
(5) Ruiz, E.; Cano, J.; Alvarez, S.; Alemany, P. *J. Am. Chem. Soc.* **1998**, *120*, 11122.
(6) (a) Abu-Youssef, M. A. M.; Escuer, A.; Gatteschi, D.; Goher, M. A. S.; Mautner, F. A.; Vicente, R. *Inorg. Chem.* **1999**, *38*, 5716. (b) Manson, J. L.; Arif, A. M.; Miller, J. S. *Chem. Commun.* **1999**, 1479.
(7) Escuer, A.; Vicente, R.; Goher, M. A. S.; Mautner, F. A. *Inorg. Chem.* **1998**, *37*, 782.
(8) Cortes, R.; Drillon, M.; Solans, X.; Lezama, L.; Rojo, T. *Inorg. Chem.* **1997**, *36*, 677.
(9) Abu-Youssef, M.; Escuer, A.; Goher, M. A. S.; Mautner, F. A.; Vicente, R. *Eur. J. Inorg. Chem.* **1999**, 687.
(10) Abu-Youssef, M.; Escuer, A.; Goher, M. A. S.; Mautner, F. A.; Vicente, R. *J. Chem. Soc., Dalton Trans.* **2000**, 413.
(11) Abu-Youssef, M.; Escuer, A.; Goher, M. A. S.; Mautner, F. A.; Reiss, G.; Vicente, R. *Angew. Chem.* **2000**, *112*, 1681; *Angew. Chem., Int. Ed. Engl.* **2000**, *39*, 1624.

10.1021/ic000516j CCC: $19.00
Published on Web 10/13/2000

Chart 1

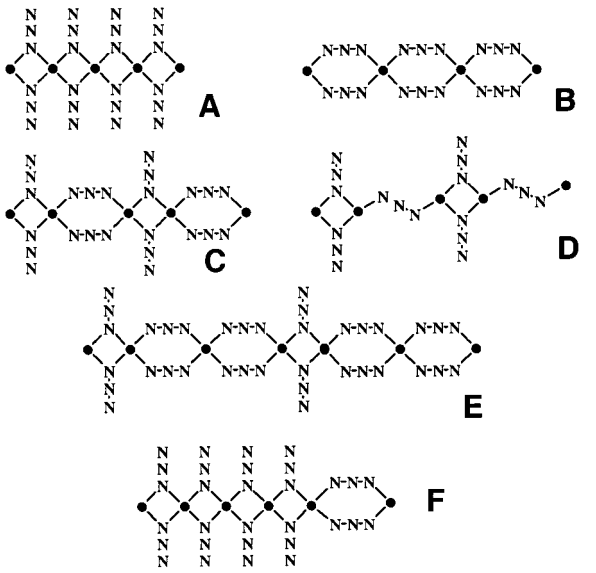

sequence (topology **E**). Susceptibility and magnetization measurements indicate that these new compounds exhibit a ferrimagnetic-like behavior with a ground-state $S = {}^5/_2$ per Mn_3 basic unit.

Molecular ferrimagnetic chains, so-called bimetallic chains, have been defined by O. Kahn as *"systems in which two kinds of magnetic centers A and B regularly alternate and the interaction parameter is negative"*.[12] Regular and alternating ferrimagnets are differentiated, but they are always referred to as heterometallic exchange-coupled systems. This agrees with the usual definition, whatever the dimensionality of the network: *"a ferrimagnet contains two different magnetic ions with near-neighbor antiferromagnetic exchange coupling"*.[13] Basically, the title compounds do not fall into this definition, since they exhibit homometallic chains, and the sign of the interaction alternates according to the AF/AF/F sequence. A similar ferrimagnetic system was reported by Escuer et al. for the chain $[Cu(Cl\text{-}py)_2(N_3)_2]_n$, showing AF/AF/F/F interactions.[14] Further, Drillon et al. have already reported the first 1-D ferrimagnet of topological origin in the homometallic compounds $A_3Cu_3(PO_4)_4$ (A = Ca, Sr), the behavior of which was analyzed in terms of the quantum chain of trimeric Cu^{II} units.[15] It should be pointed out that in these cases, some of the superexchange interactions were found to be through semicoordinative positions of the Cu^{II} ions and then the ferrimagnetic phenomenon appears only at low temperature.

On the basis of the experimental data, and the appropriate analytical expression deduced for the chains under consideration, we deduce the relevant exchange constants for **1** and **2** and we discuss the theoretical behavior for some selected values of the ratio between both interactions.

Experimental Section

Spectral and Magnetic Measurements. Infrared spectra (4000−200 cm^{-1}) were recorded from KBr pellets on a Perkin-Elmer 380-B spectrophotometer. Susceptibility measurements were performed with a Quantum Design instrument with a superconducting quantum interference device (SQUID) detector working in the temperature range 300−2 K under an external magnetic field of 100 G. Magnetization measurements were performed at 2 K up to 5 T of magnetic field. Diamagnetic corrections were estimated from Pascal tables. EPR spectra were recorded at X-band frequency with a Bruker ES200 spectrometer.

Table 1. Crystal Data and Structure Refinement for $[Mn(3\text{-}Mepy)_2(N_3)_2]_n$ (**1**) and $[Mn(3,4\text{-}Dmepy)_2(N_3)_2]_n$ (**2**)

	1	**2**
chemical formula	$C_{12}H_{14}MnN_8$	$C_{14}H_{18}MnN_8$
fw	325.25	353.30
space group	$P2_1/n$	$P\bar{1}$
a, Å	11.201(3)	11.502(4)
b, Å	14.499(4)	14.246(5)
c, Å	14.308(4)	16.200(8)
α, deg.	90	84.17(3)
β, deg.	91.87(2)	84.87(3)
γ, deg.	90	71.33(3)
V, $Å^3$	2233.1(11)	2497.2(17)
Z	6	6
temp, °C	25(2)	25(2)
λ (Mo Kα), Å	0.710 69	0.710 69
d_{calc}, $g{\cdot}cm^{-3}$	1.451	1.410
μ (Mo Kα), mm^{-1}	0.893	0.805
R^a	0.0363	0.0574
$R_w{}^{2\,b}$	0.0839	0.1077

[a] $R(F_o) = \sum||F_o| - |F_c||/\sum|F_o|$. [b] $R_w(F_o)^2 = \{\sum[(w((F_o)^2 - (F_c)^2)^2]/\sum[(w((F_o)^4]\}^{1/2}$.

Synthesis. $[Mn(3\text{-}Mepy)_2(N_3)_2]_n$ (**1**) was synthesized by mixing a methanolic solution (30 mL) of manganese(II) chloride tetrahydrate (0.99 g, 5 mmol) and 0.93 g (10 mmol) of 3-methylpyridine dissolved in 10 mL of methanol, followed by dropwise addition of a saturated aqueous solution of sodium azide (0.65 g, 10 mmol). The final solution was filtered off after 24 h and was left to stand in a dark place for 2 weeks, which led to the growth of X-ray quality greenish crystals of **1**. Yield: ca. 60%. Anal. Calcd for $MnC_{12}H_{14}N_8$: C, 44.3; H, 4.3; N, 34.5; Mn, 16.9. Found: C, 44.4; H, 4.2; N, 34.6; Mn, 16.8.

$[Mn(3,4\text{-}Dmepy)_2(N_3)_2]_n$ (**2**) was synthesized by mixing an aqueous methanolic solution (2:1, 60 mL) of manganese perchlorate hexahydrate (1.49 g, 5 mmol) and (1.07 g, 10 mmol) 3,4-dimethylpyridine dissolved in 20 mL of methanol, followed by dropwise addition of a concentrated aqueous solution of sodium azide (0.65 g, 10 mmol). The resulting turbid solution was filtered off to give a clear colorless solution that was left to stand in a dark place for several days. Green crystals suitable for X-ray determination were formed of complex **2**. Yield: ca. 80%. Anal. Calcd for $MnC_{14}H_{18}N_8$: C, 47.6; H, 5.1; N, 31.7; Mn, 15.6. Found: C, 47.7; H, 5.1; N, 31.6; Mn, 15.6.

IR Spectra. In addition to the bands of the 3-methylpyridine and 3,4- dimethylpyridine, very strong bands corresponding to the characteristic ν_{as} of the azido ligands appeared at 2072 and 2056 cm^{-1} for **1** and at 2107, 2071, and 2053 cm^{-1} for **2**.

X-ray Crystallograpy of $[Mn(3\text{-}Mepy)_2(N_3)_2]_n$ (1) and $[Mn(3,4\text{-}Dmepy)_2(N_3)_2]_n$ (2). The X-ray single-crystal data for both compounds were collected on a modified STOE four-circle diffractometer. Crystal sizes are 0.50 mm × 0.28 mm × 0.15 mm for **1** and 0.50 mm × 0.24 mm × 0.15 mm for **2**. The crystallographic data, the conditions for the intensity data collection, and some features of the structure refinements are listed in Table 1. Graphite-monochromatized Mo Kα radiation (λ = 0.710 69 Å) and the ω-scan technique were used to collect the data sets. Accurate unit-cell parameters were determined from the automatic centering of 48 reflections ($9.2° < \theta < 15.4°$) for **1** and 32 reflections ($11.0° < \theta < 14.9°$) for **2** and refined by least-squares methods. A total of 4887 reflections (3929 independent reflections, $R_{int} = 0.0209$) were collected for **1** in the range $2.81° < \theta < 25.00°$ and 9786 reflections (8780 independent reflections; $R_{int} = 0.0296$) for **2** in the range $2.75° < \theta < 25.00$. During the data collection, intensity decays of 6% of two standard reflections (2 1 0; −4 1 3) in the case of **1** and 23% of two standard reflections (3 3 1; 2 4 1) in the case of **2**, were observed. Corrections were applied for Lorentz polarization effects, for intensity decay, and for absorption using the

(12) Kahn, O. In *Molecular Magnetism*; VCH Publishers Inc.: New York, 1993.
(13) Day, P. *J. Chem. Soc., Dalton Trans.* **1997**, 701−705.
(14) Escuer, A.; Vicente, R.; El Fallah, M. S.; Goher, M. A. S.; Mautner, F. A. *Inorg. Chem.* **1998**, *37*, 4466.
(15) Drillon, M.; Belaiche, M.; Legoll, P.; Aride, J.; Boukhari, A.; Moqine, A. *J. Magn. Magn. Mater.* **1993**, *128*, 83.

Table 2. Selected Bond Lengths (Å) and Angles (deg) for $[Mn(3\text{-}Mepy)_2(N_3)_2]_n$ (**1**)

Manganese Environment			
Mn(1)···Mn(1A)	3.4724(11)	Mn(1)···Mn(2)	5.4397(16)
Mn(1)−N(21)	2.228(2)	Mn(1)−N(11)	2.260(2)
Mn(1)−N(11A)	2.229(2)	Mn(1)−N(31)	2.237(2)
Mn(1)−N(2)	2.265(2)	Mn(1)−N(1)	2.301(2)
Mn(2)−N(33B)	2.236(2)	Mn(2)−N(33)	2.236(2)
Mn(2)−N(23B)	2.246(2)	Mn(2)−N(23)	2.246(2)
Mn(2)−N(3B)	2.251(2)	Mn(2)−N(3)	2.251(2)
N(21)−Mn(1)−N(11A)	98.34(8)	N(21)−Mn(1)−N(31)	93.33(9)
N(11A)−Mn(1)−N(31)	168.29(8)	N(21)−Mn(1)−N(11)	176.24(8)
N(11A)−Mn(1)−N(11)	78.64(8)	N(31)−Mn(1)−N(11)	89.66(8)
N(21)−Mn(1)−N(2)	88.19(8)	N(11A)−Mn(1)−N(2)	88.47(8)
N(31)−Mn(1)−N(2)	91.02(9)	N(11)−Mn(1)−N(2)	89.49(8)
N(21)−Mn(1)−N(1)	88.18(8)	N(11A)−Mn(1)−N(1)	94.13(8)
N(31)−Mn(1)−N(1)	87.09(8)	N(11)−Mn(1)−N(1)	94.24(7)
N(2)−Mn(1)−N(1)	175.80(8)	N(33B)−Mn(2)−N(33)	180.0
N(33)−Mn(2)−N(23)	88.23(9)	N(23B)−Mn(2)−N(23)	180.0
N(33)−Mn(2)−N(3B)	90.28(8)	N(23)−Mn(2)−N(3)	89.36(8)
N(3B)−Mn(2)−N(3)	180.0	Mn(2)···Mn(1)···Mn(1A)	172.29(2)
Azido Bridges			
N(11)−N(12)	1.191(3)	N(12)−N(13)	1.150(3)
N(21)−N(22)	1.169(3)	N(22)−N(23)	1.161(3)
N(31)−N(32)	1.168(3)	N(32)−N(33)	1.168(3)
N(12)−N(11)−Mn(1A)	128.6(2)	N(12)−N(11)−Mn(1)	123.0(2)
Mn(1A)−N(11)−Mn(1)	101.36(8)	N(13)−N(12)−N(11)	179.2(3)
N(22)−N(21)−Mn(1)	126.6(2)	N(23)−N(22)−N(21)	177.4(2)
N(22)−N(23)−Mn(2)	136.7(2)	N(32)−N(31)−Mn(1)	130.7(2)
N(33)−N(32)−N(31)	177.8(2)	N(32)−N(33)−Mn(2)	133.0(2)

DIFABS[16] computer program (range of normalized transmission factors: 0.456−1.000 for **1** and 0.447−1.000 for **2**). The structures were solved by direct methods using the SHELXS-86[17] computer program and refined by full-matrix least-squares methods on F^2 for **2**, using the SHELXL-93[18] program incorporated in the SHELXTL/PC, V 5.03[19] program library and the graphics program PLUTON.[20] All non-hydrogen atoms were refined anisotropically. The hydrogen atoms were located on calculated positions (C_{ar}−H = 0.930 Å; C_{Me}−H = 0.960 Å), and their isotropic displacement factors were set to 1.2 times the value of the equivalent isotropic displacement parameter of the corresponding parent carbon atom. The final R indices were 0.0363 and 0.0574, respectively, for all observed reflections. The number of refined parameters was 289 (**1**) and 634 (**2**). Maximum and minimum peaks in the final difference Fourier syntheses were 0.205 and −0.220 e Å^{-3} (**1**) and 0.292 and −0.435 e Å^{-3} (**2**). Significant bond parameters for **1** and **2** are given in Tables 2 and 3, respectively.

Description of the Structures. The two compounds show similar features including the trans coordination of the pyridinic ligands, the double azido bridges between neighboring manganese atoms, and the alternating disposition of the EE or EO bridges. Therefore, some minor differences in the structural data, mainly those related to the bridging region, are described separately for each compound.

Structure of the $[Mn(3\text{-}Mepy)_2(N_3)_2]_n$ (1) Compound. A labeled ORTEP plot of the asymmetric unit is shown in Figure 1. The structure consists of neutral, well-isolated chains of manganese atoms bridged by means of double azide bridges along the (0 0 1) direction of the cell. Manganese atoms show a quite regular octahedral polyhedron with the 3-methylpyridine ligands coordinated in trans arrangement. The azido bridges show an alternating Mn(1B)−$(EE)_2$−Mn(2)−$(EE)_2$−Mn(1)−$(EO)_2$−Mn(1A) sequence in which each set of EE double azido bridges becomes equivalent because of the inversion center placed on Mn(2). The Mn(1)−$(EO)_2$−Mn(1A) subunit shows a planar centrosymmetric Mn(1)−N(11)−N(11A)−Mn(1A) ring with the Mn(1)−N(11)−Mn(1A) bond angles of 101.36(8)°. The azido ligand N(11)−N(12)−N(13) determines an angle of 22.5(2)° with the above plane, and as usual for the EO bridge, the N−N distances are clearly asymmetric, with N(11)−N(12) being larger than N(12)−N(13). The Mn(2)−$(\mu_{1,3}\text{-}N_3)_2$−Mn(1) subunit shows that the two azide bridges are practically coplanar and that the manganese atoms are out of the azide plane (0.357(1) Å for Mn(2) and 0.412(1) Å for Mn(1)), giving a chair distortion, which may be quantified with a δ parameter[7] of 12.8(1)° and 15.6(1)° for Mn(2) and Mn(1), respectively. The Mn−N−N bond angles in this unit lie in the 126.6°−136.7° range, which may considered normal for bridges of this kind. Mn···Mn intrachain distances are 5.440(2) Å (EE bridges) and 3.472(1) Å (EO bridges). The minimum interchain Mn···Mn distance is 8.865(2) Å.

Structure of the $[Mn(3,4\text{-}Dmepy)_2(N_3)_2]_n$ (2) Compound. A labeled ORTEP plot of the asymmetric unit is shown in Figure 2. The structure consists of neutral, well-isolated chains of manganese atoms bridged by means of double azide bridges along the (0 1 0) direction of the cell. The main difference with **1** is the absence in this case of inversion centers on the manganese atoms or the $Mn_2(\mu_{1,1}\text{-}N_3)_2$ subunit. The Mn−N−N bond angles involved in the end-to-end bridging region lie between 121.4° and 138.2°, in a range similar to those in **1**. The Mn−N−Mn bond angles in the end-on bridging region are Mn(1)−N(11)−Mn(2) = 99.7(2)° and Mn(1)−N(21)−Mn(2) = 101.1(2)°. The Mn−$(\mu_{1,3}\text{-}N_3)_2$−Mn subunits also show asymmetric chair distortion, with δ 13.0(2)°/22.4(2)° for the ring that includes Mn(2) and Mn(3), and 10.0(2)°/20.0(2)° for the ring that includes Mn(3) and Mn(1B). Intrachain Mn···Mn distances are Mn(2)···Mn(3) = 5.399(3) Å, Mn(3)···Mn(1B) = 5.436(3) Å (EE bridges), and Mn(1)···Mn(2) = 3.451(2) Å (EO bridges). Minimum Mn···Mn interchain distance is 8.906(5) Å.

Experimental Magnetic Data

The magnetic behavior of compounds **1** and **2**, plotted as $\chi_M T$ vs T is shown in Figure 3. As suggested by their similar topologies and bond parameters, the magnetic behavior of the two compounds is quite similar; $\chi_M T$ at room temperature is 3.63 (3.87) cm^3 K mol^{-1} for compound **1** (compound **2**). On cooling, $\chi_M T$ falls to 2.01 (2.18) cm^3 K mol^{-1} at 40 (38) K and then rises at lower temperatures to reach a maximum value of 13.1 (7.8) cm^3 K mol^{-1} at 2 K. This magnetic behavior shows the typical characteristics of ferrimagnetism, indicating a high-spin ground state. To characterize the ground state of these chains, magnetization measurements were performed at 2 K under magnetic fields up to 5 T. Magnetization data for both compounds indicate a saturation value close to 1.7 e$^-$ per manganese atom (Figure 4). This value agrees with a $S = {}^5/_2$ spin state per $[Mn_3(L)_6(N_3)_6]$ basic unit.

EPR spectra measured at room temperature were similar for both compounds; the main signal for each compound corresponds to the isotropic absorption at $g = 2.00$, with a peak-to-peak line width of 124 G for **1** and 154 G for **2**. The two compounds also exhibit weak half-field signals partially overlapping with the main signal. The line width of the $g = 2.00$ signal is greater than the value reported for chains with only EE double bridges (topology **B**, typically around 50 G) and is smaller than that for chains with alternating EE/EO double bridges (topology **C**, 300−500 G range) and for only EO bridges (topology **A**, 750 G). The reason lies in the relative intensity of two factors; exchange narrowing is more effective for EE than for EO bridges according to the coupling constant values, in the order **B** > **E** > **C** > **A**. In contrast, the opposite dipolar broadening effects, negligible for EE bridges, increase in the order **B** < **E** < **C** < **A** because of the short Mn···Mn distances within the EO bridging region.[21]

(16) Walker, N.; Stuart, D. *Acta Crystallogr.* **1983**, *A39*, 158.
(17) Sheldrick, G. M. *SHELXS-86, Program for the Solution of Crystal Structure*; University of Göttingen: Göttingen, Germany, 1986.
(18) Sheldrick, G. M. *SHELXL-93, Program for the Refinement of Crystal Structure*; University of Göttingen: Göttingen, Germany, 1993.
(19) *SHELXTL 5.03, Program library for the Solution and Molecular Graphics*, PC version; Siemens Analytical Instruments Division: Madison, WI, 1995.
(20) Spek, A. L. *PLUTON-92*; University of Utrecht: Utrecht, The Netherlands, 1992.

Table 3. Selected Bond Lengths (Å) and Angles (deg) for $[Mn(3,4\text{-}Dmepy)_2(N_3)_2]_n$ (**2**)

		Manganese Environment	
Mn(1)···Mn(2)	3.451(2)	Mn(2)···Mn(3)	5.399(2)
Mn(3)···Mn(1B)	5.436(2)	Mn(1)−N(21)	2.226(4)
Mn(1)−N(63)	2.234(4)	Mn(1)−N(53)	2.240(4)
Mn(1)−N(1)	2.258(4)	Mn(1)−N(11)	2.269(4)
Mn(1)−N(2)	2.304(4)	Mn(2)−N(31)	2.231(4)
Mn(2)−N(21)	2.243(4)	Mn(2)−N(11)	2.245(4)
Mn(2)−N(41)	2.254(4)	Mn(2)−N(4)	2.265(4)
Mn(2)−N(3)	2.268(4)	Mn(3)−N(33)	2.226(4)
Mn(3)−N(51)	2.227(4)	Mn(3)−N(43)	2.252(4)
Mn(3)−N(5)	2.273(4)	Mn(3)−N(61)	2.275(4)
Mn(3)−N(6)	2.284(4)		
Mn(1)···Mn(2)···Mn(3)	171.34(2)	Mn(2)···Mn(3)···Mn(1B)	170.98(2)
Mn(2)···Mn(1)···Mn(3A)	178.65(2)	N(21)−Mn(1)−N(63)	94.1(2)
N(21)−Mn(1)−N(53)	172.7(2)	N(63)−Mn(1)−N(53)	93.2(2)
N(21)−Mn(1)−N(1)	92.4(1)	N(63)−Mn(1)−N(1)	90.9(2)
N(53)−Mn(1)−N(1)	86.3(2)	N(21)−Mn(1)−N(11)	79.5(1)
N(63)−Mn(1)−N(11)	173.5(1)	N(53)−Mn(1)−N(11)	93.3(2)
N(1)−Mn(1)−N(11)	90.0(1)	N(21)−Mn(1)−N(2)	94.8(1)
N(63)−Mn(1)−N(2)	92.3(2)	N(53)−Mn(1)−N(2)	86.0(2)
N(1)−Mn(1)−N(2)	171.9(1)	N(11)−Mn(1)−N(2)	87.6(1)
N(31)−Mn(2)−N(21)	177.7(2)	N(3 1)−Mn(2)−N(11)	98.8(2)
N(21)−Mn(2)−N(11)	79.6(1)	N(31)−Mn(2)−N(41)	93.2(2)
N(21)−Mn(2)−N(41)	88.4(1)	N(11)−Mn(2)−N(41)	168.0(1)
N(31)−Mn(2)−N(4)	88.1(1)	N(21)−Mn(2)−N(4)	93.5(1)
N(11)−Mn(2)−N(4)	88.5(1)	N(41)−Mn(2)−N(4)	91.6(2)
N(31)−Mn(2)−N(3)	86.4(2)	N(21)−Mn(2)−N(3)	91.9(1)
N(11)−Mn(2)−N(3)	92.0(1)	N(41)−Mn(2)−N(3)	89.1(2)
N(4)−Mn(2)−N(3)	174.5(1)	N(33)−Mn(3)−N(51)	88.3(2)
N(33)−Mn(3)−N(43)	88.0(2)	N(51)−Mn(3)−N(43)	176.2(2)
N(33)−Mn(3)−N(5)	90.1(2)	N(51)−Mn(3)−N(5)	89.5(2)
N(43)−Mn(3)−N(5)	89.8(2)	N(33)−Mn(3)−N(61)	175.0(2)
N(51)−Mn(3)−N(61)	87.1(2)	N(43)−Mn(3)−N(61)	96.6(2)
N(5)−Mn(3)−N(61)	87.9(2)	N(33)−Mn(3)−N(6)	94.3(2)
N(51)−Mn(3)−N(6)	92.0(2)	N(43)−Mn(3)−N(6)	89.0(2)
N(5)−Mn(3)−N(6)	175.4(1)	N(61)−Mn(3)−N(6)	87.8(2)
		Azido Bridges	
N(11)−N(12)	1.198(5)	N(12)−N(13)	1.160(6)
N(21)−N(22)	1.208(5)	N(22)−N(23)	1.149(5)
N(31)−N(32)	1.172(5)	N(32)−N(33)	1.166(5)
N(41)−N(42)	1.170(5)	N(42)−N(43)	1.174(5)
N(52)−N(53)	1.164(5)	N(52)−N(51A)	1.172(5)
N(61)−N(62)	1.173(5)	N(62)−N(63B)	1.171(5)
N(12)−N(11)−Mn(2)	129.8(3)	N(12)−N(11)−Mn(1)	124.5(3)
Mn(2)−N(11)−Mn(1)	99.7(2)	N(13)−N(12)−N(11)	179.2(6)
N(22)−N(21)−Mn(1)	126.9(3)	N(22)−N(21)−Mn(2)	119.6(3)
Mn(1)−N(21)−Mn(2)	101.1(2)	N(23)−N(22)−N(21)	179.7(5)
N(32)−N(31)−Mn(2)	121.4(3)	N(33)−N(32)−N(31)	178.0(5)
N(32)−N(33)−Mn(3)	138.2(4)	N(42)−N(41)−Mn(2)	136.9(3)
N(41)−N(42)−N(43)	178.0(5)	N(42)−N(43)−Mn(3)	125.8(4)
N(52B)−N(51)−Mn(3)	136.6(4)	N(53)−N(52)−N(51A)	177.2(5)
N(52)−N(53)−Mn(1)	128.6(4)	N(62)−N(61)−Mn(3)	129.5(3)
N(61)−N(62)−N(63B)	177.7(5)	N(62A)−N(63)−Mn(1)	129.1(3)

Coupling Constant Determination and Discussion

Prior to this study, no analytical expression was available for determining the exchange parameters in a 1-D Heisenberg ferrimagnet consisting of alternating interactions $J_1J_1J_2$. Furthermore, the Bonner and Fisher numerical computation method,[22] based on rings of increasing size, is not useful here because the number of required spins $S = {}^5/_2$ lies outside the range of computational possibilities. Given the spin value a convenient expression may be deduced from a classical spin model, using the spin Hamiltonian

$$H = -J_1\sum(S_{3i}S_{3i+1} + S_{3i+1}S_{3i+2}) - J_2\sum S_{3i-1}S_{3i}$$

where J_1 and J_2 stand for the exchange interactions and where the S_n are classical spin vectors. This approximation is fully justifiable when studying manganese(II) chains that exhibit large spins ($S = {}^5/_2$). The wave-vector-dependent susceptibility is

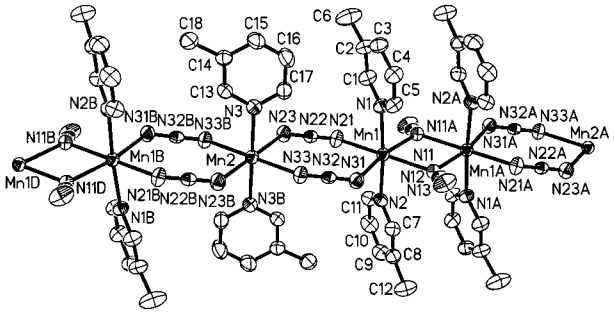

Figure 1. ORTEP drawing for *trans*-$[Mn(3\text{-}Mepy)_2(N_3)_2]_n$ (**1**). Ellipsoids are at the 40% probability level.

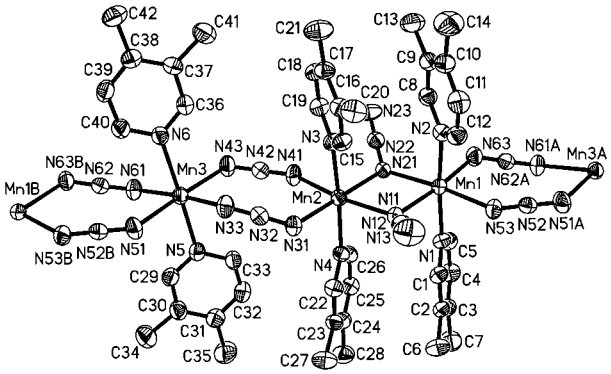

Figure 2. ORTEP drawing for *trans*-[Mn(3,4-Dmepy)$(N_3)_2]_n$ (**2**). Ellipsoids are at the 40% probability level.

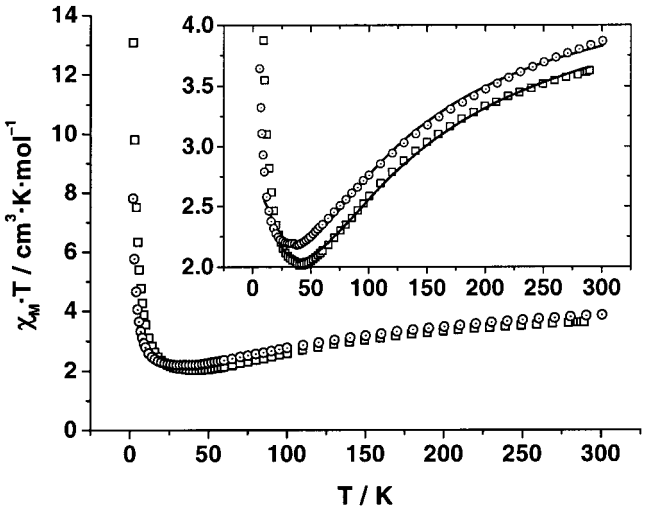

Figure 3. Plot of the molar susceptibility and $\chi_M T$ product vs T for *trans*-[Mn(3-Mepy)$_2(N_3)_2]_n$ (**1**) (open squares) and *trans*-[Mn(3,4-Dmepy)$_2(N_3)_2]_n$ (**2**) (dot-centered circles). Inset shows the details of the $\chi_M T$ minimum for **1** and **2**. Solid lines show the best fit of the data according to the proposed model.

given by

$$S(q) = \frac{1}{NkT}\sum\langle S_n S_{n+p}\rangle \exp(\mathrm{i}qp)$$

which is related to the pair correlation function between operators located at sites n and $n + p$, namely,

$$\langle S_n S_{n+p}\rangle = \frac{3}{Z}\int \frac{\mathrm{d}S_1\, \mathrm{d}S_2 \ldots \mathrm{d}S_{n+1}}{(4\pi)^{n+1}} S_n{}^z S_{n+p}{}^z \exp\left(-\frac{H}{kT}\right)$$

This expression reduces,[23,24] in the limit of the uniform chain ($J_1 = J_2$), the expression

$$\langle S_n S_{n+p}\rangle = \left[\coth\left(\frac{J}{kT}\right) - \frac{kT}{J}\right]^P = u^p$$

For the alternating chain, the pair correlation function must be written as

$$\langle S_n S_{n+p}\rangle = u_1 u_1 u_2 u_1 \ldots$$

with

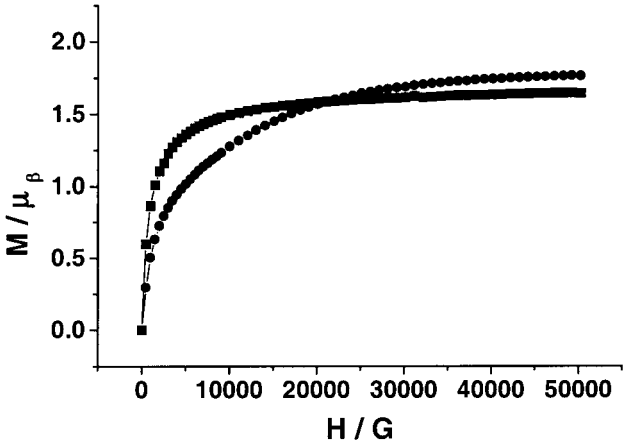

Figure 4. Magnetization curves per manganese ion for compounds **1** (solid squares) and **2** (solid circles).

$$u_i = \coth\left(\frac{J_i}{kT}\right) - \frac{kT}{J_i}$$

Taking into account the p parity, the above expression reduces to

$$S(q) = \frac{1}{kT}\{3(1 - u_1{}^4u_2{}^2) + 2(2u_1 + u_2 - u_1{}^3u_2(u_1 + 2u_2))\cos(qa) + 2(u_1{}^2 + 2u_1u_2 - 2u_1{}^3u_2 - u_1{}^2u_2{}^2)\cos(2qa)\}\{1 - 2u_1{}^2u_2\cos(3qa) + u_1{}^4u_2{}^2\}^{-1}$$

Then we obtain the expression of the bulk susceptibility, corresponding to the $q = 0$ limit, for the alternating chain $J_1J_1J_2$... as

$$\chi = \frac{C}{(1 - u_1{}^2u_2)^2}\{3(1 - u_1{}^4u_2{}^2) + 4u_1(1 - u_1{}^2u_2{}^2) + 2u_2(1 + u_1)^2(1 - u_1{}^2) + 2u_1{}^2(1 - u_2{}^2)\}$$

which reduces to the uniform chain solved by Fisher[23] for $u_1 = u_2$ (C takes the usual meaning $C = Ng^2\mu_B{}^2/(3kT)$). Such an expression differs significantly from that previously reported[8] for the alternating chain $J_1J_2J_1$.

On close examination of the $\chi T = f(T)$ data, it appears that the above compounds exhibit the typical signature of 1-D ferrimagnets, namely, a minimum of the effective moment and a divergence at low temperature, indicating exchange constants with opposite signs along the chain. To compare the theoretical expression with the experiment, we need to introduce the $J_i \rightarrow J_iS(S + 1)$ and $G \rightarrow g(S(S + 1))^{1/2}$ scaling factors. The closest agreement between theory and experiment, obtained by a least-squares refinement procedure, comes from use of the following parameter values: $J_1 = -10.5$ cm^{-1}, $J_2 = 1.37$ cm^{-1}, $g = 2.00$ for **1** and $J_1 = -10.8$ cm^{-1}, $J_2 = 0.80$ cm^{-1}, $g = 2.05$ for **2**.

The model provides a very good fit of χT variation over the temperature range 4−300 K, with a discrepancy that does not exceed experimental uncertainty. In particular, the minimum of χT and the divergence at low temperature are very well reproduced. The exchange interactions obtained with this model lie in the same range as those previously reported for azido-bridge complexes; coupling constant calculations on homogeneous manganese azido chains show that the AF interaction

(21) Bencini, A.; Gatteschi, D. *EPR of Exchange Coupled Systems*; Springer-Verlag: Berlin, Heidelberg, 1990; Chapter 10.
(22) Bonner, J. C.; Fisher, M. E. *Phys. Rew. A.* **1964**, *135*, 640.
(23) Fisher, M. E. *Am. J. Phys.* **1974**, *32*, 241.
(24) Drillon, M.; Coronado, E.; Beltran, D.; Georges, R. *Chem. Phys.* **1983**, *79*, 449.

Chart 2

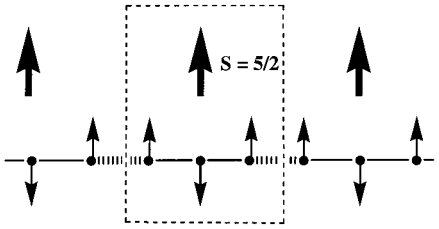

through a double end-to-end azido bridge leads to relatively high J values, within the range -7 to -13 cm^{-1}, as a function of the bond parameters.[7−9] Also, the J values reported for the double end-on azido bridges, with comparable Mn−N−Mn bond angles close to 100°, are closer to or lower than 2 cm^{-1}.

These new compounds show unprecedented magnetic properties, such as the ferrimagnetic behavior, although only one kind of spin is involved, and an apparently anomalous saturation value of $M(H)$. These properties may, in fact, be rationalized from the consideration of opposite interactions, $J_1 < 0$ (J_{AF}) and $J_2 > 0$ (J_F), and relative values $|J_{AF}| \gg J_F$. In the high-temperature limit, the influence of these interactions is negligible and $\chi_M T$ (per mol) tends to the value for isolated spins, $S = {}^5/_2$. Upon a lowering of the temperature, the moderately high J_{AF} coupling (through EE bridges) promotes the antiparallel spin configuration and a net reduction of the magnetic moment. In fact, as long as kT is high with respect to J_F, thermal disorder populates many spin configurations, including $S_T = 0$.

At very low temperature, the ferromagnetic alignment of the resulting spins (due to EO interactions) becomes efficient (Chart 2) and finally the $S_T = {}^5/_2$ spin state per Mn_3 unit is achieved, in good agreement with the saturation value of magnetization. Then the system behaves, below a threshold temperature, like a $S = {}^5/_2$ ferromagnetic chain, exhibiting a T^{-1} divergence of $\chi_M T$.

The ferrimagnetic-like behavior in these compounds clearly necessitates an even number of AF interactions followed by one or more F interactions. Simulations of the magnetic response of such systems (using $J_F = 2$ cm^{-1}) show that the temperature of the $\chi_M T$ minimum is highly dependent on the $J_F/|J_{AF}|$ ratio (Figure 5). The minimum shifts more closely toward low temperature as the AF interaction decreases. In the limit $J_F \gg |J_{AF}|$, an initial ferromagnetic-like variation is observed while at low temperature a characteristic minimum is recorded, corresponding roughly to the behavior of a (5, ${}^5/_2$) ferrimagnetic chain.

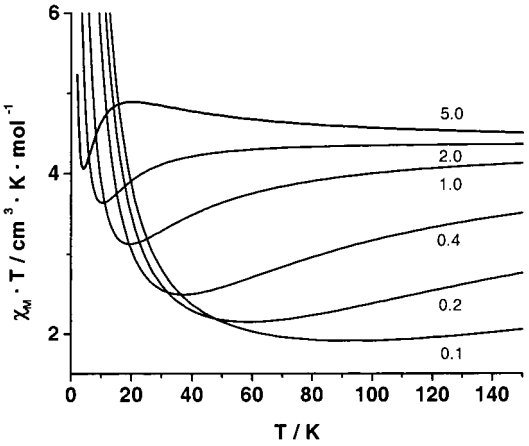

Figure 5. Simulation of the magnetic behavior of a AF/AF/F one-dimensional system for a set of the $J_F/|J_{AF}|$ ratio between 0.1 and 5.0. A constant value of $J_F = 2$ cm^{-1} has been assumed in the simulations.

Acknowledgment. This research was partially supported by CICYT (Grant PB96/0163) and OENB (Grants 6630, 7967). F. A. Mautner thanks Prof. C. Kratky and Dr. F. Belaj (University of Graz) for the use of experimental equipment.

Supporting Information Available: Two X-ray crystallographic files in CIF format. This material is available free of charge via the Internet at http://pubs.acs.org.

IC000516J